

A common De-scalping procedure for various different MRI protocols

A. Purwar¹, R. Rathore¹, R. Gupta², M. Sarma¹, G. Bayu¹, D. Rathore¹, R. Trivedi², J. Singh¹, A. Singh¹, and S. Verma¹

¹Mathematics & Statistics, IIT Kanpur, Kanpur, UP, India, ²Radiodiagnosis, SGPGIMS Lucknow, Lucknow, UP, India

Introduction: De-scalping^{1, 4} the brain is a very useful procedure with enormous applications in visualization, surface rendering, decreasing the complexity of subsequent processing algorithms, and the like. Many applications related to brain imaging either require, or benefits from the ability to accurately segment brain from the non-brain tissue. For example, (a) in the registration of b0-images to DW images in DT-MRI, both b0 and DW images often contain considerable portions of eyeballs, skin etc. that cause problems in the registration process, which gets improved once these non-brain parts of the images are removed, (b) a second application of de-scalping is in tissue-type segmentation, which helps in isolating brain tissue from other parts of the stack such as CSF, (c) in the removal of strong ghosting effects which can occur with EPI and (d) creating probabilistic atlases from large groups of subjects. This work describes an automatic procedure for de-scalping in the brain for MRI for scans with axial orientation. The procedure has effective in all types of brain imaging techniques including T1, T2W, PD, and T2W-EPI.

Materials and Methods: The method takes entire image stack, removes the scalp and returns the stripped brain part. The method starts with the user supplied slice index that has the largest part of the brain as observed by visual inspection. In absence of this input, it begins with the middle slice of the image stack. For each slice k the method works in two phases: **Phase 1: Generate Head Mask (GHM):** 1. Raw Image (Fig 1A) intensities are saturated² up to 5 % (Fig 1B). This increases the contrast level of the image. The saturated raw intensities are normalized in the 8-bit range to save computation time. 2. This is an iterative step which leaves a rough head mask: (A) Normalized raw intensities are anisotropic diffusion filtered by the edge preserving anisotropic diffusion filter proposed in [6]. (B) The resulting intensity histogram is processed to find a composite threshold (Fig 1C) using mixture modeling thresholding algorithm², which leaves a binary mask (a rough approximation of the head) (C) From this binary mask, spikes are eroded (Fig 1D) using geodesic dilation³ followed by hole-filling³ (Fig 1E). (D) From above, the largest connected component is kept as the head constitutes the single largest connected component (Fig 1F). This leaves a rough head mask for the slice k . 3. Similarity of the above head-mask is checked with the slice above or below depending on the orientation. If the level of agreement of this head-mask with the head-mask of the above slice is less than 85% using Jaccard coefficient (JC), step 2 is repeated with the refined parameters (with smoothing parameters increased by 10%) else the head mask for slice k is taken to be correct. If the head-mask segmentation was rejected 4th time, the heuristics were used to improve the segmentation result, e.g., head-mask result of the earlier slice was used as a head-mask for present slice! **Phase 2: Generate Brain Mask (GBM):** In this step, from the head-mask obtained from the procedure GHM, a rough brain mask is obtained, which is later refined in-order to get the final brain mask. The procedure works as follows: 1. The binary head-mask obtained from GHM is eroded³ (Fig 2B) with an approximate thickness of the scalp (In our experiment, 8mm for 256x256 images with FOV:240x240 mm²). This removes most of the skull part, leaving brain, and skull in the form of spikes for mid slices. 2. A rough brain mask is obtained from above. It is an iterative procedure having following steps: (I) The mask obtained from the step 1 is applied over the original filtered image (Fig 2C). This filtered image is subjected to a greyscale erosion³ (Fig 2D) (initial radius=3mm for 256x256 images with FOV:240x240 mm²) step so as to scale down those portions of the scalp which are still there. (II) From the above very bright intensity spikes are removed utilizing following criterion (Fig 2E): For each pixel, median over a circular kernel (initial radius=7mm) is obtained. If median is above a threshold, the pixel intensity under consideration is replaced by the median. (III) Above is followed by an automatic thresholding using Isodata Algorithm², dichotomizing the image into brain and background (Fig 2F). This gives a binary mask removing air and darker pixels of the scalp. Later, holes are filled via binary morphology³. (IV) Strong Connections between brain and non-brain portions, e.g., ear, nose etc. are broken using binary watershed segmentation³ on the mask obtained after thresholding (Fig 2G). Non-brain portions are removed by the procedure suggested by Atkins and Mackiewicz in [5], a brain bounding rectangle (Fig 2H) is extracted from the head mask. Only those connected components from the present mask are preserved (Fig 2I) whose centroid falls inside the brain bounding rectangle. This leaves us a mask which contains only brain portions. (V) Above mask is applied over the original filtered image, over which a grey-scale dilation³ (initial radius same as in the grey-scale erosion in step I) is performed to preserve the brain portions which have been deleted due to grey-scale erosion process (Fig 2K) in step I. 3. Above mask is subjected to correction of leakage through weak boundary. Leakage through weak boundary was detected by calculating the Jaccard coefficient between a new slice and its predecessor slice to determine their similarity. If the de-scalping for a new slice was similar to its predecessor (JC ≥ 0.85), then the de-scalping for that slice is accepted and sent for the further fine tuning of the mask. However if the de-scalping results differed (JC < 0.85), then the de-scalping for that slice is rejected, and sent for the Leakage correction which is done by changing parameter² in step 2 by 10%. The procedure is iterative. If the de-scalping was rejected 4th time, the heuristics were used to improve the de-scalping result, e.g., de-scalping result of the earlier slice was used as a rough brain mask for that slice! 4. The above mask is fine-tuned using the following procedure: One pixel thick boundary (B) of the brain mask is obtained using binary morphology. From B , an n -pixel thick inner boundary ($B_{in}(n)$) is obtained. (In our experiments, for FOV: 240x240 mm² and image size 256x256, $n = 3$ gave satisfactory results). The boundary B is tessellated with the following iterative procedure: For each pixel in B : a $(2n+1) \times (2n+1)$ rectangular window W is considered. Statistics is computed for all those pixels which are in W and $B_{in}(n)$. From the calculated statistics, pixels inside W and not in $B_{in}(n)$ that have a significant probability of coming from the distribution of interest are grown. This completes one iteration of the procedure. In our experiments, for 256x256 images with FOV:240x240 mm², 10 iterations were found enough and this number is proportional to the size of image in general. A simple growing criterion was to use $\mu \pm c \sigma$ (where μ is the mean and σ is the standard deviation (SD) with respect to the mean of the raw intensities) with $c=3.0$. This constituted an approximately 0.1% level of significance, which was found to be quite satisfactory, resulting in the final brain mask (Fig 2L). The algorithm was implemented using JAVA.

Results & Discussion: Figure 3 shows the results of present algorithm over a PD image data set. Experiments with the method did result in good extractions. However in some cases of T2 hyper-intense globe in the orbital region it failed to remove this structure. Fortunately, in such cases these extra parts are well separated from the main brain allowing a removal by a conventional paint-brush without much effort.

References: [1] Smith SM, HBM. 2002 Nov; 17(3):143-55. [2] ImageJ: <http://rsb.info.nih.gov/ij/> [3] HIPR2: <http://homepages.inf.ed.ac.uk/rbf/HIPR2/index.htm>. [4] Purwar A et al; Proc. ISMRM 14 (2006) [5] Atkins MS et al. Trans. On Med. Imaging, 17(1):98-107 (1998). [6] Tschumperlé D, et al. IEEE Trans on Pattern Analysis and Machine Intelligence, 27(4):506-517(2005).

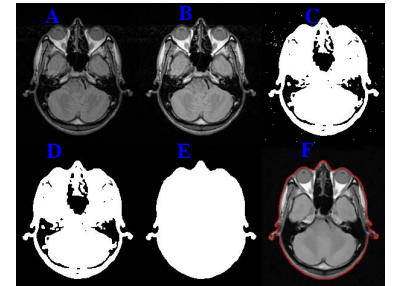


Figure 1

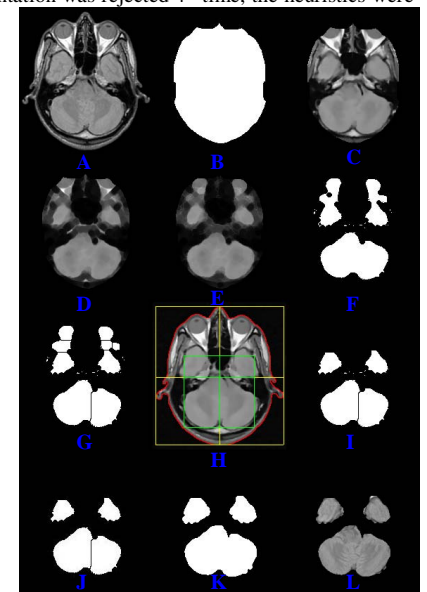


Figure 2

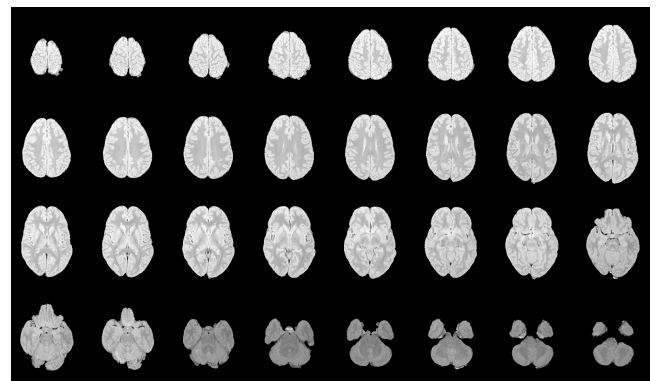


Figure 3